

# The effect of laser wavelength on the photorefractive characteristics of PMDA-DR19 based photorefractive polymeric materials

Chi-Jung Chang, Hang-Ching Wang, Ging-Yuan Liao and Wha-Tzong Whang\*

*Institute of Materials Science and Engineering, National Chiao-Tung University, 1001 Ta Hsueh Road, Hsinchu 300, Taiwan, R.O.C.*

and Jong-Ming Liu

*Materials Research Laboratories, ITRI, Hsinchu 300, Taiwan, R.O.C.*

and Ken-Yuh Hsu

*Institute of Electro-Optical Engineering, National Chiao-Tung University, 1001 Ta Hsueh Road, Hsinchu 300, Taiwan, R.O.C.*

*(Received 8 October 1996; revised 9 December 1996)*

The photoconductivity and photorefractive characteristics of PMDA-DR19-based photoconducting nonlinear optical polymeric films with different compositions were studied using red and green lasers. Contributions of dopants and the host to the photoconductive and photorefractive properties are systematically discussed. The virgin nonlinear optical material PMDA-DR19 was neither photoconductive nor photorefractive in nature. However, it became photoconductive and photorefractive once the charge transport material was incorporated into the PMDA-DR19/PVB polymer film. Films containing more nonlinear optical chromophore exhibited higher diffraction efficiency. Response speed was further elevated when an additional charge generation material was doped in. Diffraction grating was observed under zero electric field and was confirmed due to a photorefractive effect by the two-beam coupling effect. In addition to composition modification, the laser light source was also an important factor in changing the PR response speed. The photorefractive response speed was tremendously improved when films were written and read by two different laser beams, either red/green lasers or green/red lasers. © 1997 Elsevier Science Ltd.

**(Keywords: photoconductive; photorefractive; PMDA-DR19)**

## INTRODUCTION

The refractive index of photorefractive materials can be modulated by the electro-optic effect under non-uniform illumination induced space charge field. Therefore, such materials have potential applications in simulation of neural networks, phase conjugation, optical information storage and processing, and real-time holography.

The photorefractive (PR) effect of inorganic crystals such as LiNbO<sub>3</sub>, KNbO<sub>3</sub>, BaTiO<sub>3</sub>, and SBN has been widely studied during the past twenty years<sup>1–3</sup>. However, the difficulties in the crystal growth and processing limited their applications. The PR effect in an organic material was first observed in 1990<sup>4,5</sup>. The growth of doped organic crystal is also a difficult process. Polymeric PR materials seemed to be more feasible because of their attractive characteristics including high electro-optic coefficients, low dielectric constants,

versatility in selecting the charge generating and transporting materials as well as the nonlinear optical materials, and good processability<sup>6</sup>. Up to the present, three approaches have been studied to provide the required functionality including nonlinear optical polymer hosts doped with photoconducting molecules<sup>7–14</sup>, photoconducting polymer hosts doped with nonlinear optical molecules<sup>15–21</sup>, and fully functionalized polymers in which the photoconducting moiety and the nonlinear optical chromophore were attached onto the polymer chains<sup>22–26</sup>. All the photoconductivities were observed under an applied electric field. Usually, the photorefractivity was measured by applying an electric field on the target materials. Recently, Yu *et al.*<sup>29</sup> reported the photorefractivity of a fully functionalized polymer with large optical gain under zero-field condition. The photorefractivity in this report was evidenced by two-beam coupling experiments. In addition to the optical gain, the response time is also an important characteristic of the photorefractivity. According to the literature, the response time of the photorefractivity was affected by

\* To whom correspondence should be addressed

the applied electric field on the film and the composition of the films.

In our study, we design a type of photorefractive polymeric material containing two photorefractive active components with different visible spectrum absorption. According to the reported literature, the

photorefractive characteristics are improved by adjusting the chemical structure or composition of the polymeric materials. We think it is important to find the effect of the wavelength of the writing and reading beams on the photorefractivity. The PR properties are measured under zero external electric field by

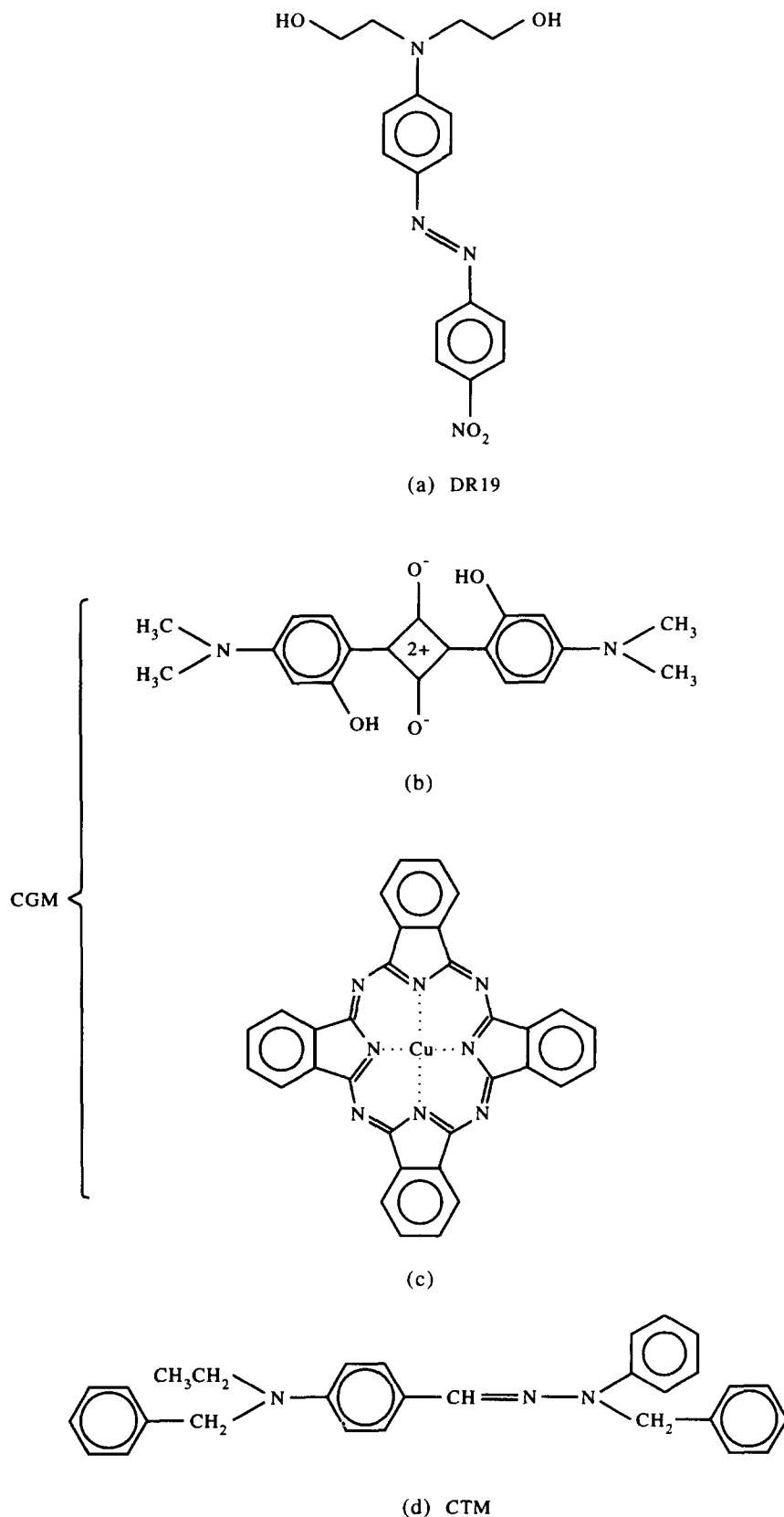


**Figure 1** Chemical structures of (a) dispersed red 19, (b) bis(4-dimethylamino-2-hydroxyl-phenyl) squaraine, (c) Cu phthalocyanine, and (d) *N*-(benzyl)-*N*-(ethyl)-benzaldehyde *N*-(benzyl)-*N*-(phenyl) hydrazone

two-beam coupling and four-wave mixing. The nonlinear optical polymer PMDA-DR19 and a charge generation material (CGM) with different visible light absorption spectrum incorporated with a charge transport material (CTM) were used to prepare the PR film. The results show that choosing appropriate writing and reading laser beams can speed up the response time of PR polymeric materials. The photorefractive characteristics of PMDA-DR19 based films will be discussed in this paper.

## EXPERIMENTAL

Synthesis of disperse red 19 (DR19), and polymerization of pyromellitic anhydride (PMDA) with DR19 are the same as those reported by us elsewhere<sup>27</sup>.

### Film preparation

The charge generation materials (CGM) including the squaraine and the Cu phthalocyanine (1:1 by weight) shown in *Figures 1b* and *c*, and the charge transfer material (CTM) illustrated in *Figure 1d* were obtained from the Material Research Laboratories of ITRI. Three types of the polymer films were prepared in this study, including (1) PMDA-DR19/polyvinylbutyral (PVB), (2)

PMDA-DR19/PVB/CTM, and (3) PMDA-DR19/PVB/CGM/CTM. Their compositions are listed in *Table 1*. Cyclohexanone was used as a solvent. The solid content of all the mixtures was set at 20 wt%. The mixture was stirred at 70°C for 12 h. PVB could aid the dispersion of CGM in the solution, but it did not cause any significant photoconductive or photorefractive effect. The PR polymeric films were prepared by spin-coating on ITO glasses with a thickness of 25  $\mu\text{m}$ .

### Physical measurement

Degenerate four-wave mixing as shown in *Figure 2* was used to generate a diffraction grating in the polymeric PR film and to read the grating. Two mutually coherent s-polarized writing beams were spatially overlapped in the polymer film with an angle between them and form a diffraction grating. A s-polarized reading beam was counterpropagating to one of the writing beams and satisfied the Bragg condition. The angle between the writing beams was of 14°. A red beam laser ( $\lambda = 632.8 \text{ nm}$ ) and a green beam laser ( $\lambda = 514 \text{ nm}$ ) were applied as writing beams or a reading beam alternately. All the PR signals were measured without applying electric field across the film.

For photoconductivity measurement, gold was

**Table 1** Compositions of the solid content in the solution used for spin coating of PMDA-DR19-based polymeric films

Film	PMDA-DR19 10% solution	CGM 10% solution	CTM 10% solution	Final solid content <sup>a</sup>
PMDA-DR19/PVB	20 parts			20%
PMDA-DR19/PVB/CTM	20 parts		50 parts	20%
PMDA-DR19/PVB/CGM/CTM (I)	20 parts	1 part	50 parts	20%
PMDA-DR19/PVB/CGM/CTM (II)	5 parts	1 part	50 parts	20%

<sup>a</sup> Solid content adjusted by addition of the PVB into the solution

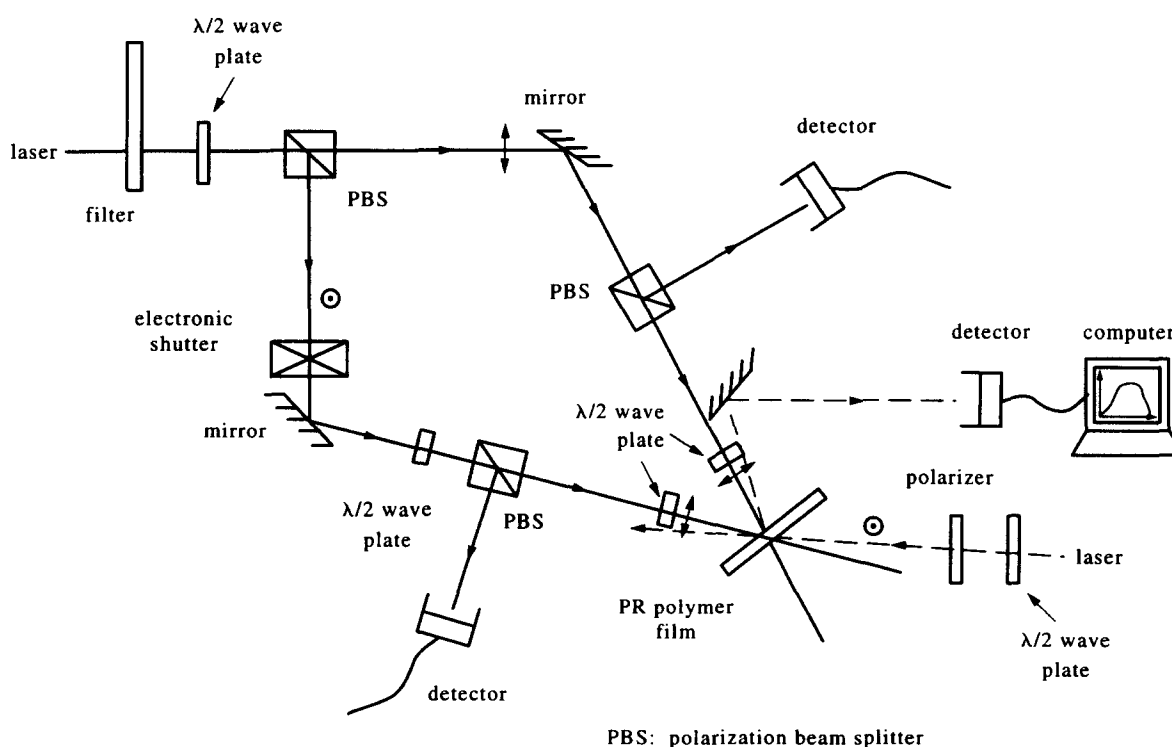


**Figure 2** Experimental setup of the degenerate four-wave mixing measurement

vapour-deposited on the PR polymer film spin-coated onto indium–tin oxide (ITO) glasses. A red beam laser ( $\lambda = 632.8 \text{ nm}$ ) and a green beam laser ( $\lambda = 514 \text{ nm}$ ) were chosen as light sources with a fixed power intensity ( $20 \text{ mW mm}^{-2}$ ) to measure the photoconductivity of the polymer under the fixed applied field (300 V).

In the two beam coupling measurement as demonstrated in Figure 3, a green laser beam with wavelength 514 nm was selected as the light source. It was split into two beams which were termed as S (signal) and P (pump) with equal intensity. These two incident beams intersected in the polymeric film to form an interference pattern. By chopping one of the beams, the transmitted intensity of the other beam could be measured.

*Structure characterization*

The u.v./vis spectra of the samples dissolved in cyclohexanone were recorded with a Hitachi-U2000 u.v./vis spectrometer. Thermal analysis was performed

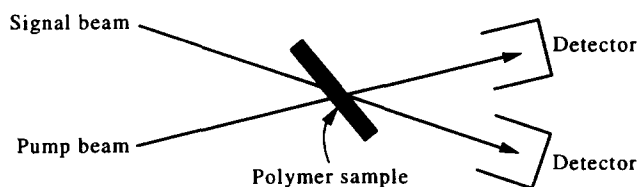


Figure 3 Experimental setup of the two-beam coupling measurement

using a TA DSC 2910 at a heating rate of  $10^\circ\text{C min}^{-1}$  under a nitrogen stream. The glass transition temperature of PMDA-DR19 was found at  $112^\circ\text{C}$ .

RESULTS AND DISCUSSION

The u.v./vis spectra of CTM, CGM, PMDA-DR19, PMDA-DR19/PVB/CTM and PMDA-DR19/PVB/CGM/CTM are shown in Figure 4. CGM, CTM and the NLO chromophore have maximum absorptions at different wavelengths. There was an absorption plateau between 350 and 410 nm for CTM. The CTM did not show significant absorption above 410 nm. The absorption peak for CGM and PMDA-DR19 were at 644 and 486 nm, respectively. Since the absorption peak of CGM showed a shoulder toward 500 nm, an overlap between the absorption peaks of CGM and PMDA-DR19 was observed in the spectrum of PMDA-DR19/PVB/CGM/CTM.

*Photoconductive characteristics*

Since NLO component and CGM component exhibited different absorption peaks at 486 nm (green light) and at 644 nm (red light) respectively, polymeric films with different compositions were exposed by two lasers (514 and 632.8 nm wavelengths) to study the contributions of individual components to the photoconductivity behaviour. The photocurrent responses of the PMDA-DR19/PVB, PMDA-DR19/PVB/CTM, PMDA-DR19/PVB/CGM/CTM films exposed by a red light laser and a

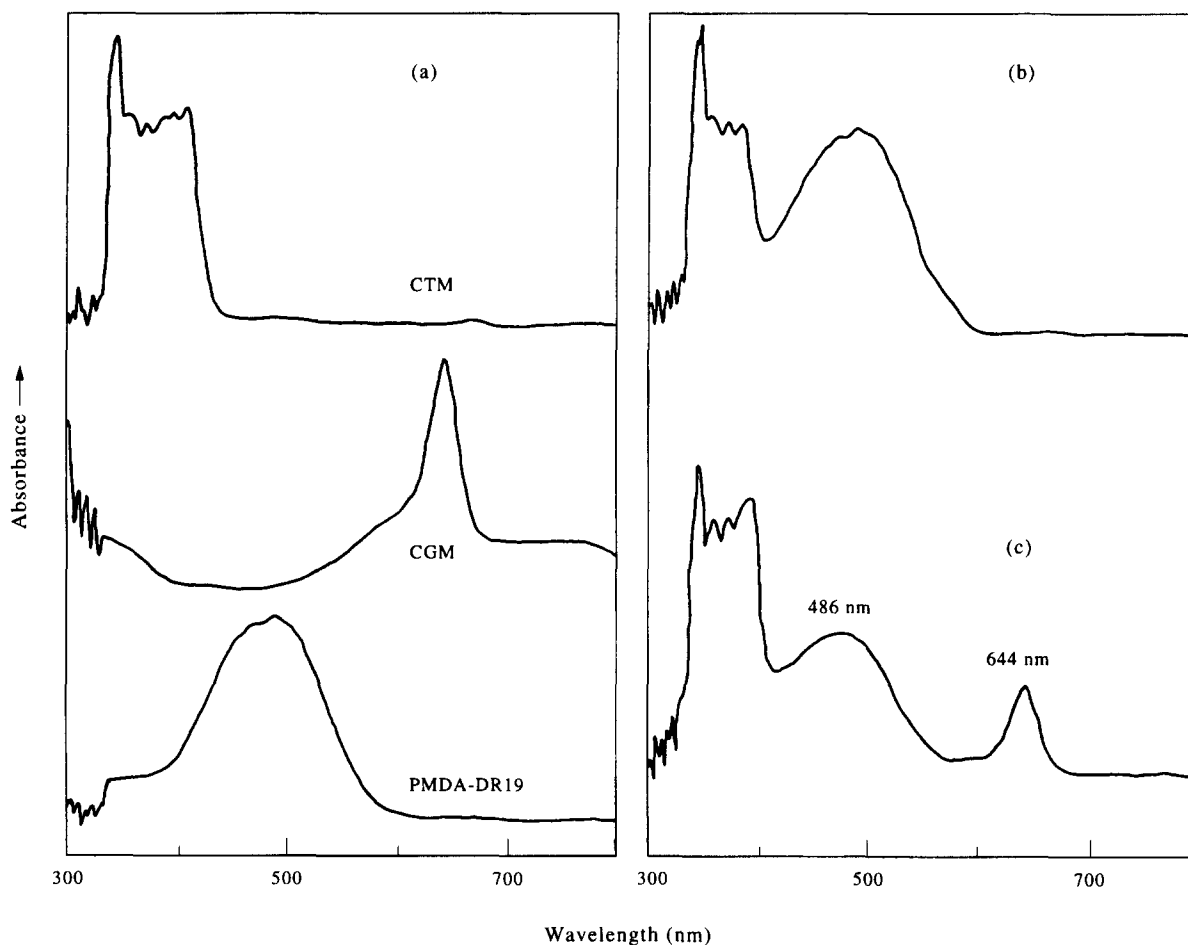
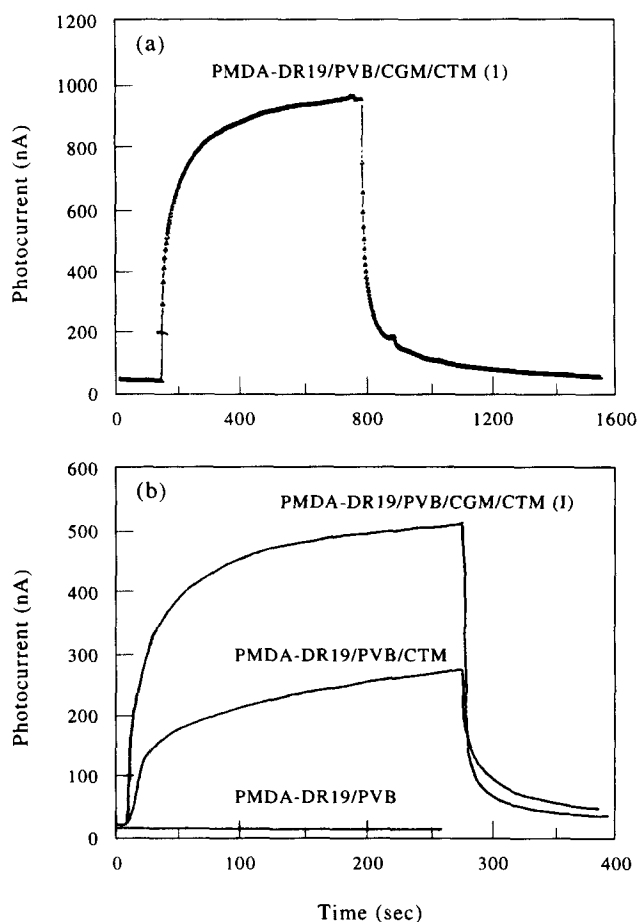
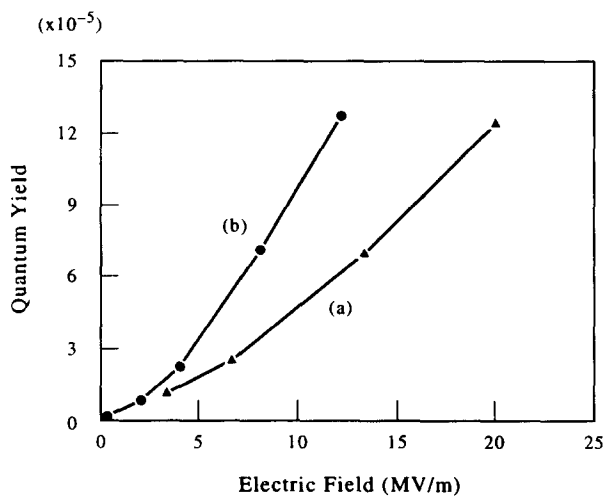


Figure 4 U.v. spectra of (a) the individual components including PMDA-DR19, CGM, and CTM, (b) PMDA-DR19/PVB/CTM, and (c) PMDA-DR19/PVB/CGM/CTM



**Figure 5** Photocurrent response of (a) the film exposed by a red laser beam ( $\lambda = 632.8$  nm) and (b) three films exposed by a green laser beam ( $\lambda = 514$  nm) under an applied voltage of 300 V



**Figure 6** Electric field dependence of quantum efficiency for the photocharge carrier generation in (a) PMDA-DR19/PVB/CTM film under a green laser at 514 nm and (b) PMDA-DR19/PVB/CTM/CGM film under a red laser at 632.8 nm

green light laser are demonstrated in Figure 5. Their photoconductivity characteristics were quite different. Film containing both PMDA-DR19 and PVB binder only was not photoconductive. PVB did not have any contribution to the photoconductivity and photorefractivity. However, the PMDA-DR19/PVB/CTM films exhibited excellent photoconductivity. The addition of

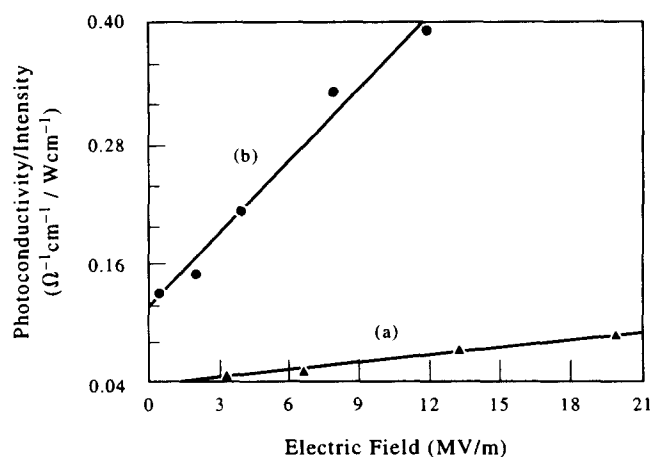


**Figure 7** Electric field dependence of photoconductivity divided by the laser intensity in (a) PMDA-DR19/PVB/CTM film under a green laser at 514 nm and (b) PMDA-DR19/PVB/CTM/CGM film under a red laser at 632.8 nm

CTM induced the generation of photocurrent. It seemed that the NLO species, PMDA-DR19, acted as a photogenerator in the presence of CTM. Figure 5a showed that addition of the fourth component, CGM, resulted in a much greater photocurrent. Figures 5a and b show the influence of incident light on the photocurrents of PMDA-DR19/PVB/CTM films. The PR film exposed by the red laser showed a higher photocurrent than those exposed by the green laser because the maximum absorption of CGM was in the red light region. The field dependent quantum efficiency,  $\Phi$ , for production of a charge carrier per absorbed photon can be calculated from<sup>30</sup>:

$$\Phi = j/(eN)$$

where  $j$  is the photocurrent density and  $N$  is the number of photons absorbed per unit time and area.  $N$  can be calculated from the energy of the laser beam and the absorption coefficient of the samples at the wavelength of the laser beam derived from the u.v./vis spectra. The quantum yield of PMDA-DR19/PVB/CTM exposed by green light lasers, and PMDA-DR19/PVB/CTM/CGM films exposed by red light lasers are demonstrated in Figure 6. The quantum yield increased with increasing strength of external electric field in both cases. Such field dependence of the quantum efficiency can be explained by the Onsager theory. Besides, the quantum yield of the latter was higher than that of the former under the same electric field. It might result from closer wavelengths between CGM absorption and the incident red light than those between PMDA-DR19 absorption and the incident green light.

The field dependence of the photoconductivity of PMDA-DR19/PVB/CTM and PMDA-DR19/PVB/CTM/CGM films normalized by the laser intensity are shown in Figure 7. In each case, the photoconductivity increased as the applied electric field increased. Meanwhile, films containing CGM exhibited higher photoconductivity than those without CGM. Since the mole ratio of the PMDA-DR19 component to the CGM is about 13, the higher quantum yield and photoconductivity in PMDA-DR19/PVB/CTM/CGM films means that CGM exhibits a higher charge generating efficiency and/or acts as an excellent energy transfer material.

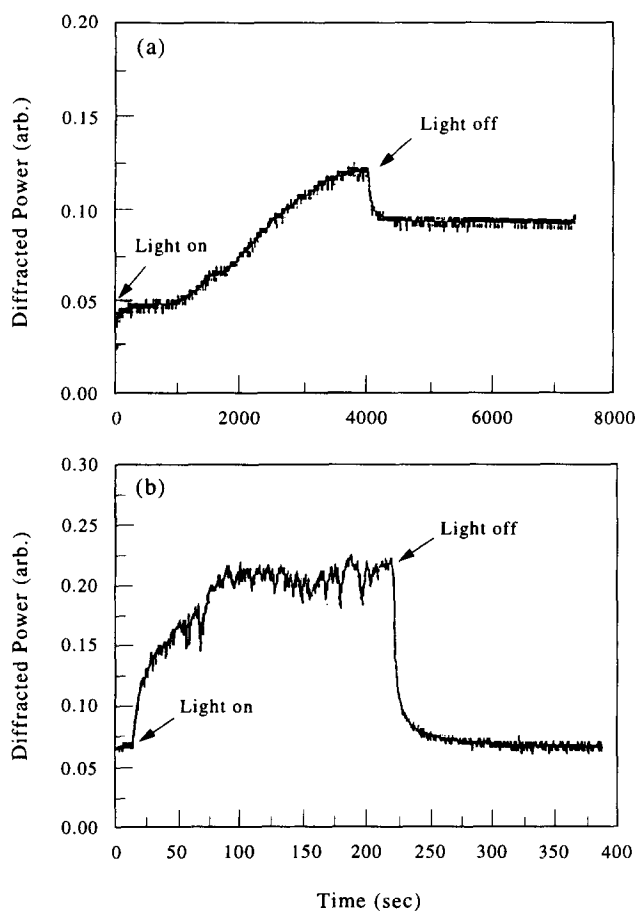
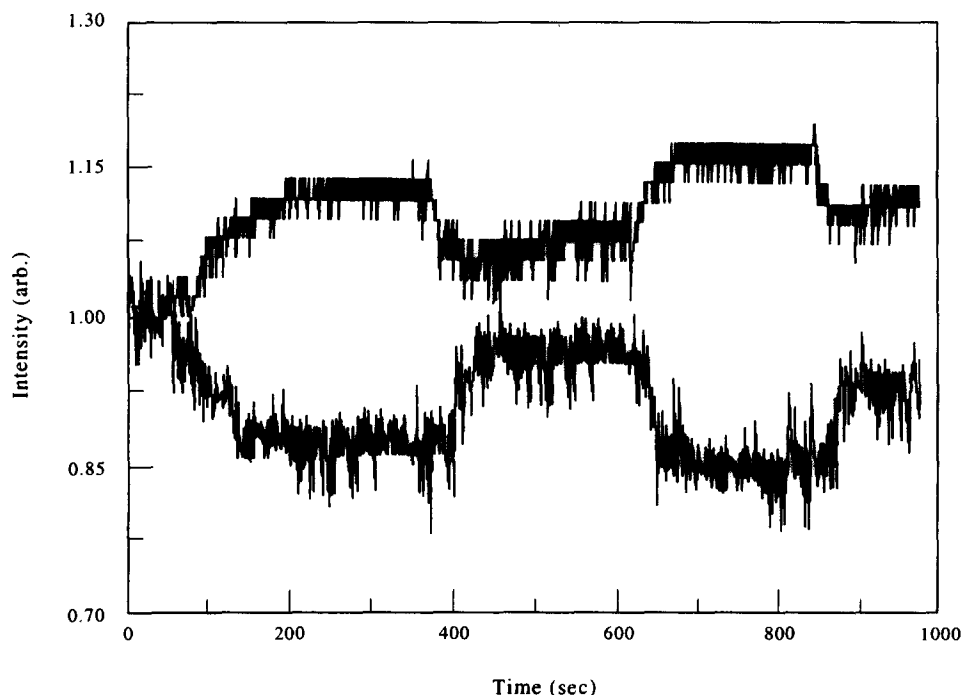


**Figure 8** Four-wave mixing diffraction signal of (a) PMDA-DR19/PVB film and (b) PMDA-DR19/PVB/CTM film written by a green laser beam ( $\lambda = 514 \text{ nm}$ ,  $10 \text{ mW mm}^{-2}$ ) and read by a red laser beam ( $\lambda = 632.8 \text{ nm}$ ,  $2.23 \text{ mW mm}^{-2}$ ) without any external electric field

*Photorefractive properties*

For understanding photorefractive characteristics, it is important to define the 'rise time' ( $T_r$ ) of the PR grating formation and the 'decay time' ( $T_d$ ) of the PR grating erasure. Before being read by a reading beam, the diffraction grating is first formed by two writing beams coherently meeting together in the film. The grating can be erased once one of the writing beam is cut off.  $T_r$  is defined as the time required for the diffraction signal intensity to rise from 10 to 90% of the steady state value, and  $T_d$  is defined as the time required for the signal to drop from 90 to 10% of the steady state value after the writing beam is removed.

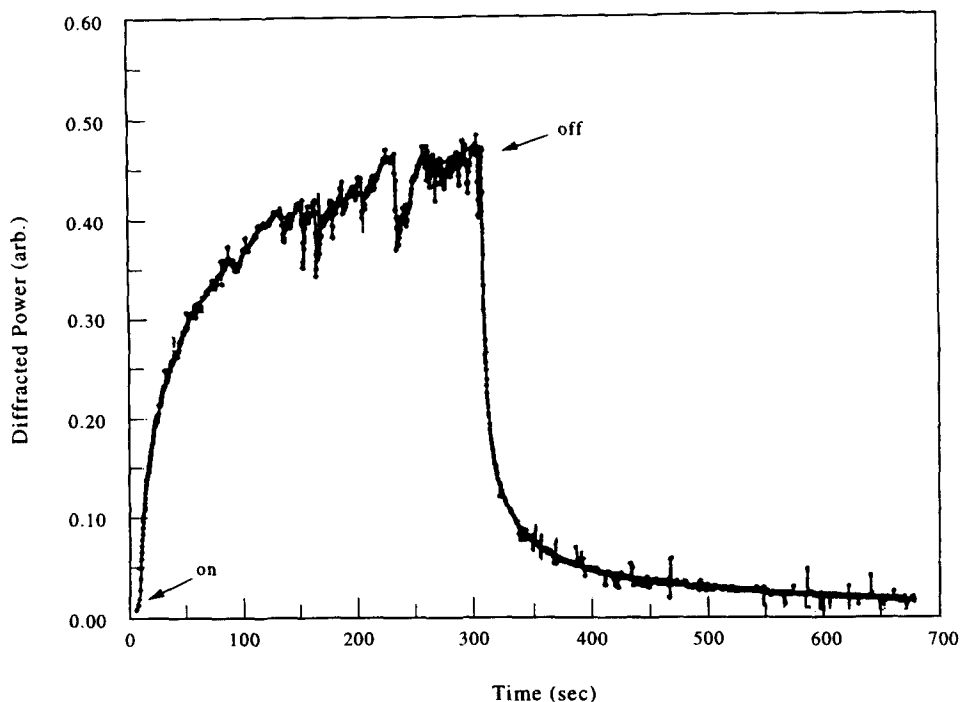
Since the CTM dopant modified the properties of the PMDA-DR19 film from nonphotoconductive to photoconductive, the diffraction phenomena of these two films were quite different in nature as shown in Figure 8. Figure 8a illustrated the diffraction signal response of the PMDA-DR19/PVB film written by two 514 nm green laser beams and read by a red laser beam. The diffraction light intensity increased gradually and had not reached a saturation value after 4400 s. In addition to the PR effect, the local temperature variation of the film can also result in the refractive index variation, leading to a grating. Since the diffraction light intensity of the film increased slowly and the film was short of photoconductivity, the slow diffraction response might be attributed to local temperature changes of the film due to absorption of incident light beams. The diffraction signal responses of the PMDA-DR19/PVB/CTM film written by a green light laser and read by a red light laser are demonstrated in Figure 8b. The addition of CTM made the films photorefractive. The diffraction response behaviours of PMDA-DR19/PVB/CTM was quite different from that shown in Figure 8a. The response speed of films with CTM was much faster than that of films without CTM, the diffraction signal raised immediately and soon reached a steady value during writing and dropped



**Figure 9** Changes in the transmitted beam intensities in the two-beam coupling experiment when pump beam is on and off. Top: Intensity of beam 1; bottom: intensity of beam 2

**Table 2** Photorefractive response time and diffraction efficiency of two PMDA-DR19-based photorefractive polymeric films

Film denotation	Writing beam	Reading beam	$T_r$ (s)	$\eta$
PMDA-DR19/PVB/CGM/CTM (I)	red (632.8 nm)	red (632.8 nm)	130	$10^{-3}$
	green (514 nm)	red (632.8 nm)	1.1	$10^{-3}$
PMDA-DR19/PVB/CGM/CTM (II)	red (632.8 nm)	red (632.8 nm)	1500	$10^{-4}$
	red (632.8 nm)	green (543 nm)	5.2	$10^{-4}$

**Figure 10** PR diffracted signal of the PMDA-DR19/PVB/CGM/CTM films (I) written and read by a red laser beam ( $\lambda = 632.8$  nm) with light intensities 10 and  $2.23 \text{ mW mm}^{-2}$ , respectively, without any external electric field

quickly to a steady value upon erasure.  $T_r$  and  $T_d$  were 80 s and 20 s, respectively, for PMDA-DR19/PVB/CTM film written by the green light laser beam.

The u.v./vis absorption plateau of CTM lies between 350 and 410 nm. Addition of CTM did not increase the absorption of green laser light (514 nm) and had little influence on the local temperature variation as those discussed in the previous paragraph. Such a promotion in response speed was evidence that the diffraction signal was due to PR effect. Further evidence for the photorefractive effect was confirmed using two-beam coupling (2BC) experiments. Figure 9 shows the 2BC signal for the PMDA-DR19/PVB/CTM film measured from two successive experiments under zero electric field. In the first experiment, the intensity of beam 1 was monitored as beam 2 was switched on and off. In the second experiment, the intensity of beam 2 was monitored as beam 1 was switched on and off. An increase in the intensity of beam 1 and a similar decrease in beam 2 indicated an asymmetric energy transfer from one beam to another when the PR films were exposed by the incident beams. In addition to the photorefractive (PR) effect, some effects (photochromism, thermochromism, thermorefractive, etc.) also showed the diffraction grating. But only PR effects gave rise to a  $90^\circ$  phase shift between the incident light intensity pattern and the refractive index modulation. Therefore, diffraction data measured in this study were caused by the PR effect.

When CGM (squaraine) was incorporated into the film, both PMDA-DR19 and squaraine could act as charge generator. Two kinds of photorefractive PMDA-DR19/PVB/CGM/CTM films with different PMDA-DR19 contents were prepared as shown in Table 1. The composition of film II was the same as film I except that the amount of PMDA-DR19 in film II was less than in film I. The PR properties of film I and film II written and read by different light sources are listed in Table 2. The diffraction efficiency of film I containing more PMDA-DR19 was higher than that of film II. The content of PMDA-DR19 in the photorefractive films exhibited significant influences on the diffraction efficiency.

The diffraction signal response of film I which was written/read by the red/red beams and green/red beams was illustrated in Figures 10 and 11, respectively. The diffraction efficiencies calculated from Figures 10 and 11 was of the same order ( $10^{-3}$ ). As for the response time, both  $T_r$  and  $T_d$  of PMDA-DR19/PVB/CGM/CTM films were much shorter than those of PMDA-DR19/PVB/CTM films. The response speed was promoted remarkably when CGM was incorporated although both films had the same diffraction efficiency at the steady state. As already shown in Figure 7, the photoconductivity of the PMDA-DR19/PVB/CGM/CTM film was higher than that of the PMDA-DR19/PVB/CTM film. The higher photoconductivity was able to create a higher

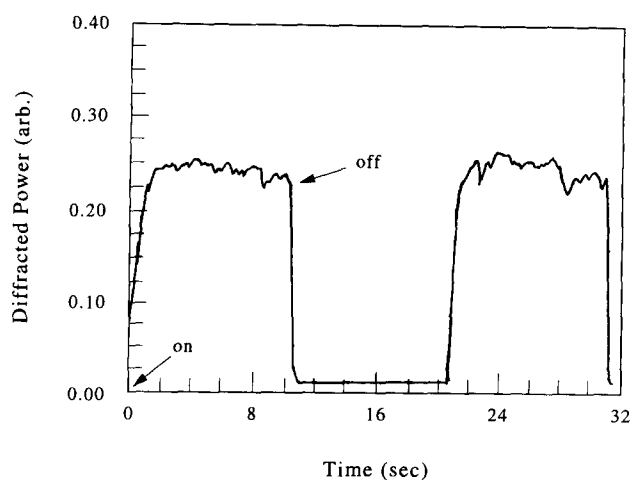


**Figure 11** PR diffraction signal of the PMDA-DR19/PVB/CGM/CTM films (I) written by a green laser beam ( $\lambda = 514 \text{ nm}$ ,  $10 \text{ mW mm}^{-2}$ ) and read by a red laser beam ( $\lambda = 632.8 \text{ nm}$ ,  $2.23 \text{ mW mm}^{-2}$ ) without any external electric field

space charge field and to speed up the response speed. In addition, both films I and II exhibited much faster response speed when they were written or read by the green light laser beams compared with those written and read by the red beams. Since the u.v./vis maximum absorption of the NLO chromophores is within the green light region and the CGM showed a shoulder with lower absorption in the same region. The green incident lights excited the NLO chromophore to generate charges near its neighbouring NLO chromophores and formed a high space charge field around the NLO chromophores. Therefore, the NLO segments were easier to align, and the PR response was faster with the exposure of the writing green beams. When a green laser beam was used as a reading beam, it provided a potential photoconductive background due to the absorption of the NLO chromophores. Because the two writing red beams created a photograting in the PR film, the grating was significantly enhanced by the field-enhanced photo-carrier separation from the potential photoconductive background upon reading by a green laser. Further studies should be continued to prove the above assumption. Such a distinct promotion in the response speed resulting from using different wavelengths of laser beams for writing and reading is worth more research. It proved an easy way to improve the response time of the photorefractive polymeric material.

## CONCLUSION

The relation between the photorefractive properties and the composition of PMDA-DR19 based films was studied. The PMDA-DR19/PVB films were neither photoconductive nor photorefractive until an additional component, CTM, was incorporated into the film. Film containing more PMDA-DR19 showed higher diffraction efficiency and faster response. Adding CGM led to an elevation in response speed. Without applying an external electric field, PMDA-DR19/PVB/CTM film exhibited much faster diffraction signals than PMDA-DR19/PVB films. An asymmetric optical energy exchange was shown in the two beam coupling measurement for PMDA-DR19/PVB/CTM. It proved that the diffraction of PMDA-DR19/PVB/CTM in the

four-wave mixing measurement was attributed to PR diffraction. In the four-wave mixing measurement, the PR diffraction signal of the PMDA-DR19/PVB/CGM/CTM film responded tremendously fast by using different wavelengths for writing or reading laser beams. The additional green incident lights might help the NLO segment generate charges near its neighbouring NLO chromophores and form a greater space charge field around the NLO chromophores. It made the NLO moieties more easily aligned, and promoted the PR response speed. It might be due to the potential photoconductive background induced by the green light absorption of NLO chromophores. A further study is necessary to prove the proposed mechanism. This study not only provided a new PR polymer showing PR effect under zero electric field but also found a new way to promote the PR response speed by choosing the appropriate writing and reading light sources and by adjusting the composition of the film.

## ACKNOWLEDGMENT

We acknowledge the financial support from the National Science Council of the Republic of China under grant no. NSC 83-0208-M-009-046.

## REFERENCES

- Gunter, P. and Huiguard, J. P., (Eds), *Photorefractive Materials and Their Applications*, Vols I and II. Springer, Berlin, 1988.
- Weiss, S. and Fisher, B., *Opt. Quantum Electron.*, 1990, **22**, 517.
- Ducharme, S., Scott, J. C., Twieg, R. J. and Moerner, W. E., *Phys. Rev. Lett.*, 1991, **66**, 1846.
- Sutter, K., Hullinger, J. and Gunter, P., *Solid State Commun.*, 1990, **74**, 867.
- Sutter, K. and Gunter, P., *J. Opt. Soc. Am. B*, 1990, **7**, 2274.
- Yu, L., Chan, W., Bao, Z. and Cao, X. F., *Macromolecules*, 1993, **26**, 2216.
- Zhang, Y., Spencer, C. A., Ghosal, S. and Casstevens, M. K., *Appl. Phys. Lett.*, 1994, **64**, 1908.
- Eich, M., Reck, B., Yoon, D. Y., Willson, C. G. and Bjorklund, G. C., *J. Appl. Phys.*, 1989, **66**, 3241.
- Schildkraut, J. S., *Appl. Phys. Lett.*, 1991, **58**, 340.
- Silence, S. M., Walsh, C. A., Scott, J. C., Matray, T. J., Twieg, R. J., Hacke, F., Bjorklund, G. C. and Moerner, W. E., *Opt. Lett.*, 1992, **17**, 1107.
- Cui, Y., Zhang, Y., Prasad, P. N., Schildkraut, J. S. and Williams, D. J., *Appl. Phys. Lett.*, 1992, **61**, 2132.
- Silence, S. M., Walsh, C. A., Scott, J. C. and Moerner, W. E., *Appl. Phys. Lett.*, 1992, **61**, 2967.
- Jungbauer, D., Teraoka, I., Yoon, D. Y., Reck, B., Swalen, J. D., Twieg, R. and Willson, C. G., *J. Appl. Phys.*, 1991, **69**, 8011.
- Ducharme, S., Jones, B., Takacs, J. M. and Zhang, L., *Opt. Lett.*, 1993, **18**, 152.
- Obrzut, J., Obrzut, M. J. and Karasz, F. E., *Synth. Mater.*, 1989, **29**, E103.
- Gelsen, O. M., Bradley, D. D. C., Murata, H., Tsutsui, T., Saito, S., Ruhe, J. and Wegner, G., *Synth. Met.*, 1991, **41**, 875.
- Zhang, Y., Cui, Y. and Prasad, P. N., *Phys. Rev. B*, 1992, **46**, 9900.
- Donckers, M. C. J. M., Silence, S. M., Walsh, C. A., Hache, F., Burland, D. M., Moerner, W. E. and Twieg, R. J., *Opt. Lett.*, 1993, **18**, 1044.
- Chang, L. T., Tam, W., Marder, S. R., Stiegman, A. E., Rikken, G. and Spangler, C. W., *J. Phys. Chem.*, 1991, **95**, 10643.
- Boyd, G. T., Francis, C. V., Trend, J. E. and Ender, D. A., *J. Opt. Soc. Am. B*, 1991, **8**, 887.
- Hampsch, H. L., Yang, J., Wong, G. K. and Torkelson, J. M., *Polym. Commun.*, 1989, **30**, 40.
- Tamura, K., Padias, A. B., Jr Hall, H. K. and Peyghambarian, N., *Appl. Phys. Lett.*, 1992, **60**, 1803.



23. Kippelen, B., Tamura, K., Peyghambarian, N., Padias, A. B. and Hall, H. K. Jr., *J. Appl. Phys.*, 1993, **74**, 3617.
24. Li, J., Lee, Y. J., Yang, Y., Kumar, J. and Tripathy, S. K., *Appl. Phys.*, 1991, **B53**, 279.
25. Li, J., Jeng, R. J., Kamath, M., Kumar, J. and Tripathy, S. K., *Mater. Res. Soc. Symp. Proc.*, 1992, **277**, 160.
26. Sansome, M. J., Teng, C. C., East, A. J. and Kwiatek, M. S., *Opt. Lett.*, 1993, **18**, 1400.
27. Liao, C. L., Huang, J. Y., Chang, C. J. and Whang, W. J., *Nonlinear Optics*, 1995, **12**, 309.
28. Chen, M., Yu, L., Dalton, L. R., Shi, Y. and Steier, W. H., *Macromolecules*, 1991, **24**, 5421.
29. Yu, L., Chen, Y., Chan, W. K. and Peng, Z., *Appl. Phys. Lett.*, 1994, **64**, 9.
30. Gailberger, M. and Bassler, H., *Phys. Rev. B*, 1991, **44**, 8643.